12.8 Empirical Wave Spectra Models

We conclude our review of experimental data on the dynamic air-water surface with a discussion of certain empirical models of wind-wave spectra. These models and the ideas they represent are perhaps the single most important outgrowth of the current developments in the theory of ocean wave analysis and forecasting. The first definitive wave spectrum model to be found is that of Neumann [189] which in turn was inspired by the pioneering work of Pierson [199], and Pierson and Marks [202] in using modern generalized harmonic analysis on ocean wave records. In this section we shall briefly review the genesis of the Neumann spectrum, discuss its pertinence to the problems of hydrologic optics, review some alternate spectra that were developed subsequent to the Neumann spectrum and, finally, give an overview of the properties of one-dimensional spectra common to all current models. This overview should be helpful in eventual applied hydrologic optics studies of wind-generated seas.

The Neumann Spectrum

The Neumann spectrum for gravity waves of period τ is of the form:

$$T_\tau = \frac{1}{8} C \frac{g^2 \tau^4}{4\pi^2} \exp \left\{ -2 \left(\frac{g\tau}{2\pi U_a} \right)^2 \right\} \tag{1}$$

where

$$C = 8.27 \times 10^{-4} \text{ sec}^{-1} ,$$

and where T_τ is defined and related to the two-dimensional (directional) spectra in (113) of Sec. 12.4, g is the acceleration of gravity (980 cm sec^{-2}), and U_a is wind speed in centimeters per second and is of "*anemometer height*," which varies from 10 to 20 feet above mean sea level. The period $\tau (= 2\pi/\sigma)$ is given in units of seconds.

Figure 12.50 depicts the characteristic shape of the Neumann spectrum for several wind speeds. The ordinate corresponding to the rationalized frequency $f \mp 1/\tau$ (i.e., $2\pi f = \sigma$) is interpretable as being proportional to the amount of total wave energy per unit frequency at frequency f, over a unit horizontal area of surface (cf. (11) of Sec. 12.3) contributed by all waves passing a point on the sea surface in all possible directions. The dynamic air-water surface is understood to be in equilibrium with the wind over deep water and at the end of a long fetch.

The total area under the curves in Fig. 12.50 increases swiftly with wind speed, in fact according to the fifth power of U_a, as we shall see. Furthermore the maximum points on curves systematically move to lower frequencies (longer periods--i.e., bigger waves) with increasing U_a. This decrease, too,

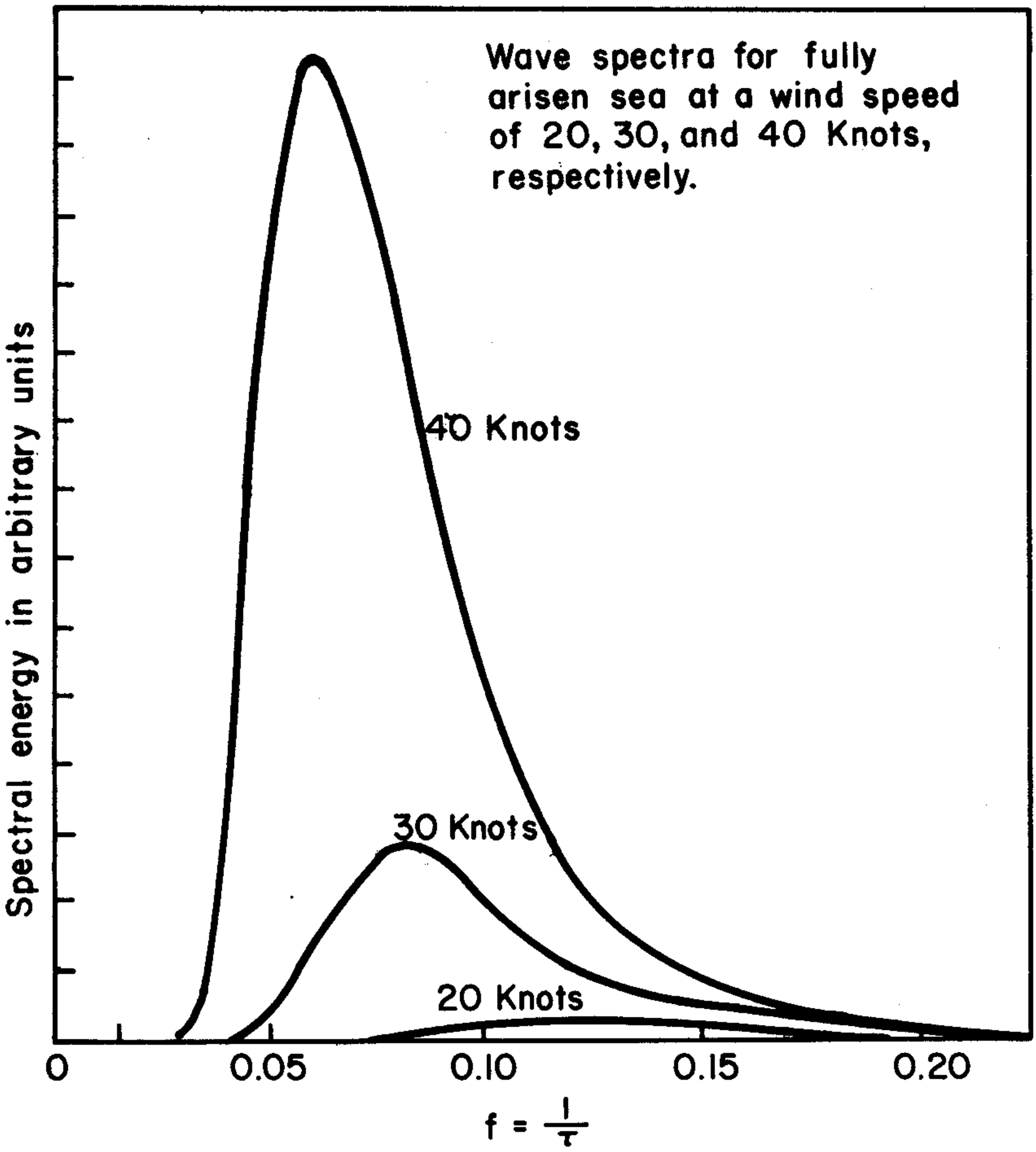

FIG. 12.50 Showing the way the wave energy spectrum increases rapidly with increasing wind speed and how the peaks descend to lower frequencies with increasing wind speed (after Neumann).

is predictable and follows a simple law such that the product of the wind speed U_a and the abscissa of the maximum is a constant. In this way, radiative transferists and others who are acquainted with classical heat radiation theory, will see a striking resemblance between the Neumann spectrum and the radiant emittance curve of a Planckian radiator. While no connections between these two types of spectra have yet been made except on an obvious intuitive statistical level, there is without a doubt a strong underlying analogy between the spectra of these two apparently dissimilar phenomena (i.e., light wave transport, ocean wave transport) and perhaps in the future some unifying theory, underlying both phenomena and yielding each spectrum as a special case, will be evolved.

Derivation of the Neumann Spectrum

A brief outline of the derivation of the Neumann spectrum, as it was originally made in [189], will be instructive for radiative transferists because it will illustrate the physical level to which the spectrum's descriptions apply. Moreover, an insight into the problem of extending the Neumann spectrum into the capillary region may possibly be forthcoming by doing so.

The Neumann spectrum is the result of observing the statistical connection between two concepts long used in empirical wave generation studies, namely the *wave steepness* and *wave age* of the dynamic air-water surface.

The *wave steepness* of an idealized sinusoidal wave form of height H and length λ is H/λ (recall that $H = 2a$ where a is the amplitude of a wave). For visual observations of the sea surface, it is customary to replace λ by the squared period τ^2, and study the alternate measure of wave steepness H/τ^2 rather than H/λ. This alternate measure is suggested by the ideal connection:

$$\lambda = \frac{g}{2\pi}\tau^2 \quad , \quad (\lambda = c\tau) \tag{2}$$

between wavelength λ and wave period τ for gravity waves in deep water. This follows from (65) and (66) of Sec. 12.3 and the connection $\tau = 2\pi/\sigma$. The real waves at sea of course do not follow idealized wave forms, but are instead viewable as the superposition of many such forms. Instead of the wave period τ, Neumann used the *apparent wave period* $\tilde{\tau}$ which is the time between successive crests on a wave record or in a visual observation at sea. Furthermore the *apparent wave height* (also denoted by "H" below) was also adopted and is defined as the average of the wave heights between two successive crests. See Fig. 12.51. From now on "H" denotes apparent wave height. It can be shown [204], [189], that a version of (2) can be defined for the *apparent wave* description. The result is:

$$\tilde{\lambda} = \frac{2}{3}\frac{g}{2\pi}\tilde{\tau}^2 \tag{3}$$

where $\tilde{\lambda}$ is now an *apparent wavelength*. Equation (3) may be thought of as an average of (2) over the wavelength pattern depicted in Fig. 12.51.

The *wave age* of an apparent wave in the air-water surface is the ratio of the wave speed (celerity) c to the wind speed U_a, namely c/U_a. The closer the ratio is to 0, the "younger" the sea. A ripe old wave age is near 1 and is attained under long-fetch, steady-wind conditions. (In Fig. 12.38, wave age is denoted by "C_o/U".)

In the study of real seas, the ideal steepness parameter H/τ^2 is replaced by $H/\tilde{\tau}^2$, and the ideal wave age c/U_a is often replaced by the apparent wave age $\tilde{\tau}/U_a$, as suggested by the

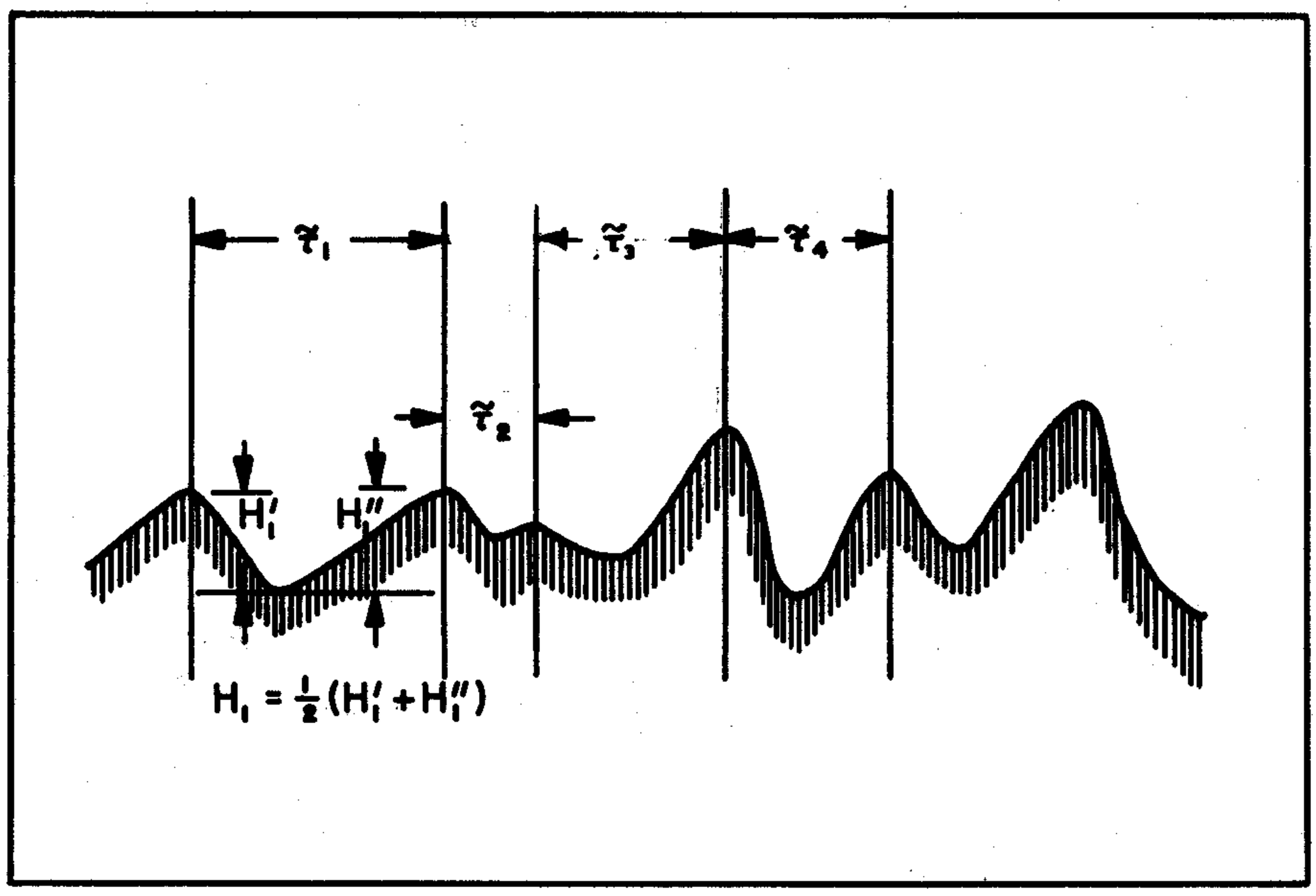

FIG. 12.51 Visual determination of apparent wave heights and apparent wave periods.

relation $c = (g/2\pi)\tau$, in its averaged form: $\tilde{c} = (g/2\pi)\tilde{\tau}$. Examples of wave steepness and wave age as used by Sverdrup and Munk, *et al.*, may be seen in Fig. 12.38 (there, however, wave height is *significant* wave height).

The results of the visual observations of the sea taken in 1948 by Neumann in Long Branch, New Jersey, are plotted in Fig. 12.52. Apparent wave steepness $H/\tilde{\tau}^2$ (measured on a logarithmic scale) in its relation to the square of apparent wave age $(\tilde{\tau}/U_a)^2$ scatters widely over the figure. It is reasonable to expect this scatter, since for a given $\tilde{\tau}/U_a$ in a steady wind, one expects all manners of steepness from very small amounts and *up to a certain limit*. The mean line of upper limits is marked by the sloping solid line in Fig. 12.52. Since the vertical scale is logarithmic the empirical relation Neumann encountered is necessarily of the form:

$$\frac{H}{\tilde{\tau}^2} = 0.219 \exp \left\{ - 2.438 \, (\tilde{\tau}/U_a)^2 \right\} . \qquad (4)$$

Neumann notes the interesting numerical closeness of 2.438 and $(g/2\pi)^2$, in which $g = 9.8$ m/sec^2. Using this and (2), Neumann wrote (4) as:

$$H = (\text{constant}) \cdot \frac{g\tilde{\tau}^2}{2\pi} \cdot \exp \left\{ - \left(\frac{g\tilde{\tau}}{2\pi U_a} \right)^2 \right\} \qquad (5)$$

where U_a is in meters per second, H in meters.

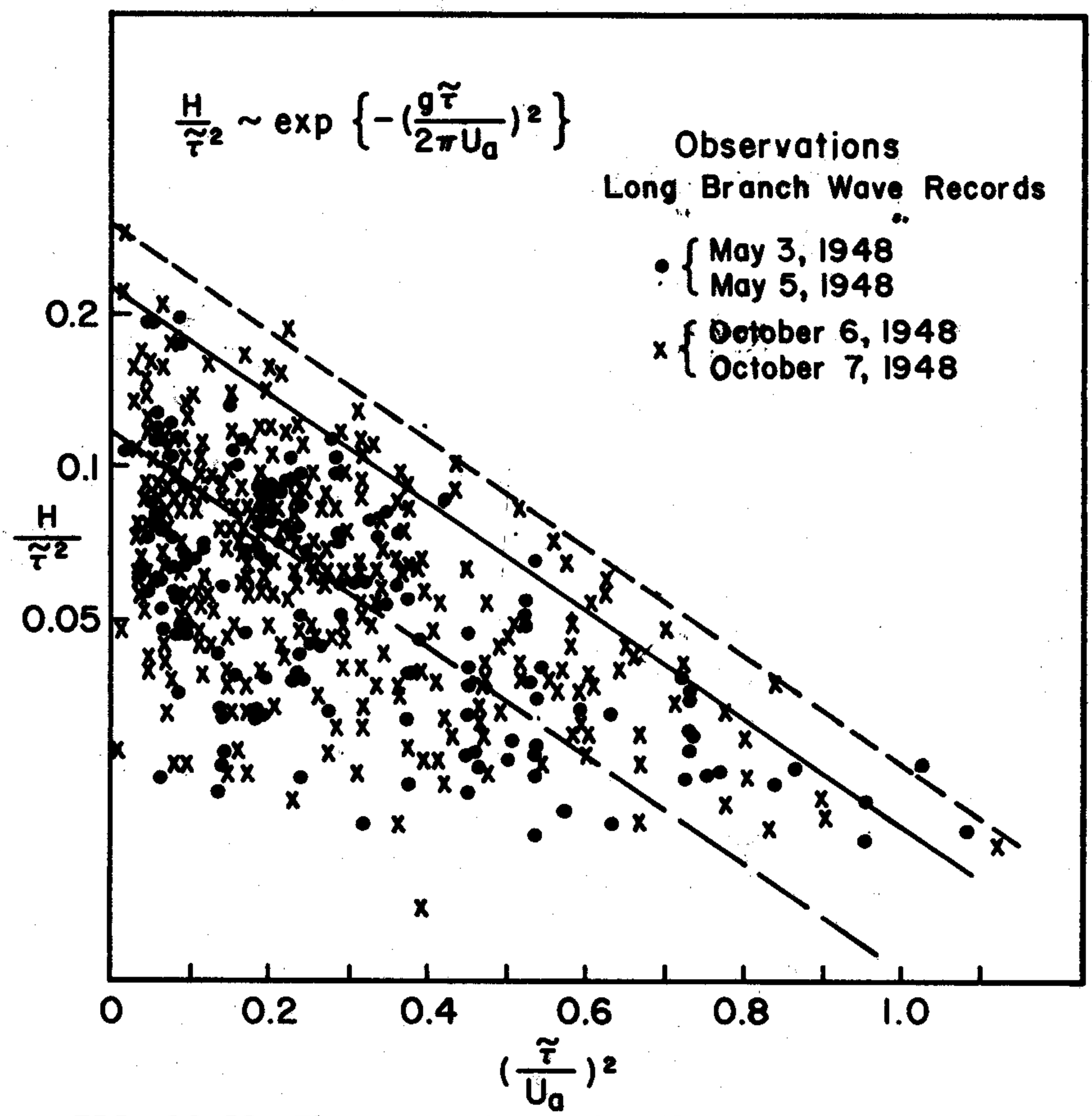

FIG. 12.52 The central result of Neumann's classic wave spectrum experiment: The semilog relation between the square of apparent wave age $(\tilde{\tau}/U_a)^2$ and apparent wave steepness $H/\tilde{\tau}^2$, leading in turn to the Neumann spectrum.

We now recall ((98) of Sec. 12.3, with $T_1 = 0$) that the energy $\mathcal{E}(\tau)$ of a *single* gravity wave of height $H(\tau)$ and period τ is:

$$\mathcal{E}(\tau) = \frac{1}{8}\rho g H^2(\tau) \quad . \tag{6}$$

This formula gives total energy (kinetic and potential) (*per unit area* of horizontal reference surface) of the dynamic sea. Neumann showed that H in (5) is an energy *density* spectrum in the sense that $H^2\, d\tau$ is proportional to the energy $\mathcal{E}(\tau)\, d\tau$ of waves per unit area on the sea with periods in the range $\tau \pm \tau \pm (1/2)\, d\tau$, and in this way arrived at the *continuous* version of (6):

$$\mathcal{E}(\tau_1,\tau_2) = \frac{1}{8}\,\rho g \int_{\tau_1}^{\tau_2} H^2(\tau)\; d\tau \qquad (7)$$

with $H(\tau)$ given by (5). Here, then, $\mathcal{E}(\tau_1,\tau_2)$ is the energy of the waves per unit horizontal area of sea surface on a fully arisen sea, and with periods in the interval $[\tau_1,\tau_2]$. Hence, by squaring each side of (5) we arrive at (1), after identifying (with Neumann) $\tilde{\tau}$ with τ for the purposes of the present derivation. Using (112) and (114) of Sec. 12.4 we can cast (1) into temporal frequency form:

$$\boxed{T_\sigma = \frac{1}{8}\,C\,g^2(2\pi)^3\,\sigma^{-6}\exp\left\{-2\left(\frac{g}{\sigma U_a}\right)^2\right\}} \qquad (8)$$

where C is the (constant)^2 of (5) and is given as in (1); U_a is in centimeters per second, g in centimeters per second squared, and σ is in radians per second (i.e., $\sigma = 2\pi/\tau$, where τ is the period). In arriving at (1), we used the relations in (98) and (103) of Sec. 12.3, along with (115) of Sec. 12.4, which yield the connection

$$\int_{\tau_1}^{\tau_2} T_\tau\; d\tau = \frac{1}{8}\int_{\tau_1}^{\tau_2} H^2(\tau)\; d\tau$$

for every pair $[\tau_1,\tau_2]$; whence:

$$T_\tau = \frac{1}{8}\,H^2(\tau) = \frac{\sigma^2}{2\pi}\,T_\sigma \qquad (8a)$$

for every τ. The constant C in (1) was determined by Neumann [189], and is closely compatible with c_1 in (6) of Sec. 12.7. The value c_1 was calculated via an alternate method by Pierson [199], and was subsequently used in the SWOP, i.e., in [45]. See also (39) in [57]. The connection that necessarily exists between them is $c_1 = (2\pi g)^2 C$.

Three Laws Derived from the Neumann Spectrum

We now consider three laws that may be derived from the Neumann spectrum (8), laws which are of help in gaining deeper insight into the structure of the graphs in Fig. 12.50 and also in providing cross-checks on the empirical spectrum itself by providing alternate theoretical and empirical approaches to the spectrum.

The first law is the temporal-frequency wind-speed *displacement law*, which relates the maximum frequency σ_{max} with the wind speed U_a. We find σ_{max} by obtaining $dT_\sigma/d\sigma$ via (8) by setting

$$\frac{dT_\sigma}{d\sigma} = 0 \quad ,$$

and by solving for the necessary value of σ. The result is

$$\sigma_{max} = \frac{\sqrt{27/3}\ g}{U_a}$$

or

$$\boxed{\sigma_{max}\ U_a = \sqrt{27/3}\ g} \quad . \tag{9}$$

Hence the frequency at which the highest density of wave energy occurs depends inversely on the generating wind speed: the greater the wind speed U_a, the smaller the maximum frequency σ_{max} --or the greater the period--or the longer the wave will be. The resemblance between (9) and the Wien displacement law derived from the Planck law of radiant emittance of an ideal blackbody is quite interesting, especially from the point of view of what concepts in the thermal radiation context pair with what in the oceanic wave context.

The second law to be derived is the *mean-elevation wind-speed law*, and this also has an interesting connection with classical thermodynamics. The Stefan-Boltzmann law of heat radiation, which states that the radiant emittance of a Planckian radiator over the whole spectrum is proportional to T^4, has the following analog in the ocean wave case. From (115) of Sec. 12.4 and (8) we have:

$$\overline{\zeta^2} = \int_0^\infty T_\sigma\, d\sigma = \frac{1}{8}\, C\, g^2 (2\pi)^3 \int_0^\infty \sigma^{-6} \exp\left\{ -2 \left(\frac{g}{\sigma U_a}\right)^2 \right\} d\sigma$$

that is:

$$\boxed{m_{oo} = \overline{\zeta^2} = \frac{3C\pi^3}{32 g^3} \sqrt{\frac{\pi}{2}}\ U_a^5} \quad . \tag{10}$$

Thus the mean square elevation of the dynamic air-water surface--as far as the gravity waves are concerned--increases as the fifth power of the wind speed U_a.

The coefficient of U_a works out to be Errata

$$\frac{3C\pi^3}{32g^3}\sqrt{\frac{\pi}{2}} = 3.2\times10^{-6}\ m^{-3}\ sec^5$$

so that

$$m_{oo} = \overline{\zeta^2} = 3.2\times10^{-6}\ U_a^5 \qquad \text{Errata}$$

when U_a is in meters per second.

The third law we shall derive from the Neumann spectrum is the *wave-slope wind-speed law* and is a special case of the wave-slope wind-speed law discovered by Duntley and corroborated by Cox and Munk (cf. (18)-(21), and (30)-(35) of Sec. 12.5). Assuming the directional spectrum $F(\sigma,\phi)$ to be isotropic, as in (127) of Sec. 12.4, we find from (128) of Sec. 12.4 and (8) above:

$$m_{20} = m_{02} = \frac{1}{2g^2}\int_0^\infty \sigma^4\ T_\sigma\ d\sigma$$

$$= \frac{C(2\pi)^3}{16}\int_0^\infty \sigma^{-2}\ \exp\left\{-2\left(\frac{g}{\sigma U_a}\right)^2\right\}d\sigma\ ,$$

so that:

$$\boxed{m_{20} = m_{02} = \frac{C\pi^3}{4g}\cdot\sqrt{\frac{\pi}{2}}\ U_a} \qquad \text{Errata} \quad (11)$$

The essential fact to observe here is that the mean square slopes increase linearly with wind speed U_a. It is for this reason that the Neumann spectrum, although derived from observations on gravity waves, seems to extend meaningfully down to the capillary-wave level. This fact was first noted by Pierson and also by Cox and Munk [57], and may be rendered in the following form using (11) and the value of C in (1):

$$\sigma_c^2 = \sigma_u^2 = 0.8\times10^{-3}\ U_a \qquad \text{Errata} \qquad (12)$$

where σ_c^2 and σ_u^2 are the cross and upwind components of the mean square slope of the surface, and U_a is in meters per second. (Compare (12) with (18)-(21) and (30)-(35) of Sec. 12.5.)

Alternate Forms of the One-Dimensional Spectrum

After the pioneering efforts of Neumann, several variants of (1) were suggested by various writers, the principal differences between the new proposed forms and (1) being in the powers to which τ was to be raised both in the algebraic factor and in the exponential factor. The great complexity of the dynamic air-water surface and the difficulty with which representative seas could be observed has left the question of the appropriate form of T_τ only partially resolved to the present time (1966). However, some recent work by Pierson and Moskowitz [203] indicates that with improved data and observing conditions, along with some powerful dimensional analysis arguments,* the form of the spectrum best suited to describe the *gravity* wave portion of the spectrum is that advocated by Bretschneider [34]:

$$T_\sigma = C\, g^2\, \sigma^{-5}\, e^{-D\left(\frac{g}{\sigma U_a}\right)^4} \tag{13}$$

where C and D are dimensionless parameters as suggested by Pierson and Moskowitz [203]:

$$C = 8.10 \times 10^{-3}$$

$$D = 0.74$$

and where the cgs system of units is used. Still further variations of the basic theme are given by:

$$T_\sigma = a\, \sigma^{-5}\, e^{-\left(\frac{b}{\sigma U_a}\right)^2} \tag{14}$$

suggested by Roll and Fischer [267]; and also:

$$T_\sigma = a\, \sigma^{-5}\, e^{-\left(\frac{b}{\sigma U_a}\right)^3} \tag{15}$$

suggested in [203]. From these forms we see that the question of the power σ^{-5} outside the exponential seems to be resolved but that the power of σ in the exponential is yet at issue. The work in [203] suggests that (13) is superior to (14) and (15), and even (8), in describing *gravity wave* spectra. In view of the multiplicity of these spectral forms, the time seems ripe for a deeper study in both observation techniques of ocean wave spectra and their theoretical basis in nonlinear hydrodynamic theory.

---

*The power of dimensional analysis in studying mathematical models of fluid flow is also illustrated, e.g., in [22].

General Properties of Gamma-Type Spectra

The Neumann spectrum (1), or (8), the Bretschneider spectrum (13), the Roll-Fischer spectrum (14) and some others of current interest are all special cases of the general type of spectrum:

$$T_\sigma = a\,\alpha^{-p}\,e^{-\left(\frac{b}{\sigma U_a}\right)^q} \qquad (16)$$

Errata

which we shall call the *gamma-type* one-dimensional spectrum, for the reason that it has the gestalt of one of the equivalent forms of the integrands used to define the gamma function of classical analysis.* There are four parameters describing a gamma-type spectrum: p and q are positive real numbers--usually integers--which define the *form* or *geometric shape* of T_σ, while a and b are respectively ordinate and abscissa scale factors with dim $a = L^2T^{1+p}$, dim $b = L\,T^{-2}$. The Neumann spectrum (8) is the special case of (16) in which $p = 6$, $q = 2$, and where $a = (1/8)\,C\,g^2(2\pi)^3$, $b = \sqrt{2}\,g$.

We shall now study some general properties of gamma-type spectra, properties which perhaps can help choose between various future special cases of (16) for particular hydrologic optics applications. We begin with the observation that the displacement law (9) holds for any T_σ of the form (16). Indeed, we find on setting

$$\frac{d\,T_\sigma}{d\sigma} = 0$$

that necessarily:

$$\sigma_{max}\,U_a = b\left(\frac{q}{p}\right)^{1/q} \qquad (17)$$

which is the displacement law for the temporal frequency σ_{max} and wind speed U_a. Hence in any of the gamma-type models proposed so far, we may expect an exact inverse relation between wind speed U_a and the maximum of the frequency wave spectrum.

We take up next the matter of deriving the general moment m_{so} of T_σ, using the definition of m_{pq} in (88) of Sec. 12.4, and the assumption of isotropy of $S(k,\phi)$ or $F(\sigma,\phi)$ ((120) of Sec. 12.4).

---

*Alternately, generalizations of T_τ given in (1) may take the form of χ^2 distributions with finite numbers of degrees of freedom.

We begin with:

$$m_{so} = \int_{E_2} E(\mathbf{k})\ u^s\ dV(\mathbf{k})$$

$$= \int_{E_2} S(k,\phi)\ u^s(k,\phi)\ d\phi\ dk$$

$$= \frac{1}{2\pi} \int_o^\infty \int_o^{2\pi} T_k\ k^s\ \cos^s\phi\ d\phi\ dk \quad .$$

It is clear that:

$$m_{so} = 0$$

for odd s. Accordingly, we shall henceforth assume that s = 2r for some nonnegative integer r. Then:

$$\boxed{m_{2r,o} = \frac{1}{\sqrt{\pi}} \frac{\Gamma\left(r + \frac{1}{2}\right)}{r!} \int_o^\infty k^{2r}\ T_k\ dk} \quad . \qquad (18)$$

We may convert this into temporal frequency form; the result is:

$$m_{2r,o} = \frac{\Gamma\left(r + \frac{1}{2}\right)}{\sqrt{\pi}\ g^{2r}\ r!} \int_o^\infty \sigma^{4r}\ T_\sigma\ d\sigma \quad . \qquad (19)$$

We can evaluate $m_{2r,o}$ in closed form when T_σ is a spectrum of the gamma type (16). The resultant form is:

$$\boxed{m_{2r,o} = \frac{a\Gamma\left(r + \frac{1}{2}\right)}{\sqrt{\pi}\, q\, g^{2r}\ r!} \left[\frac{b}{U_a}\right]^{4r-p+1} \Gamma\left(-\frac{4r - p+1}{q}\right)} \quad . \qquad (20)$$

On setting r = 0 and then r = 1 in (20) we obtain the two moments of greatest current interest in hydrologic optics, namely m_{oo}, the mean square elevation of the air-water surface; and m_{2o} the mean square slope of the surface. Thus by (89)-(91) of Sec. 12.4:

$$m_{oo} = \overline{\zeta^2} = \frac{a}{q} \left[\frac{b}{U_a}\right]^{1-p} \Gamma\left(\frac{p-1}{q}\right) \quad , \qquad (21)$$

and:

$$m_{2o} = \frac{a}{qg^2} \left[\frac{b}{U_a}\right]^{5-p} \Gamma\left(\frac{p-5}{q}\right) \qquad (22)$$

From this we see that the Neumann spectrum (the case p = 6) is the only one of the proposed spectra for gravity waves which reproduces the observed linear dependence of m_{2o} on wind speed U_a for capillary-type waves. Interestingly enough, the Bretschneider spectrum (13), for which p = 5, predicts that m_{2o} is independent of wind speed (!), and is therefore a spectrum clearly *in*applicable to the capillary wave domain. On the other hand m_{oo} for the Bretschneider spectrum increases as the fourth power of U_a, which has some experimental corroboration.

If the Neumann spectrum does well in the capillary region as regards the wave-slope wind-speed law, then we may inquire as to how well it does with respect to the higher moments of the spectrum. For example, it is known that the fourth order moments m_{4o}, m_{o4} describe the gaussian curvature of an isotropic sea surface [57], and that the mean gaussian curvature of the surface is approximated by $1/R^2$ where R is the radius of an osculating sphere in contact with the surface. Now Schooley [275], has observed from laboratory wind wave experiments that the radius R of curvature of the wind blown surface (comprised mostly of short gravity waves and long capillary waves, i.e., waves in the transitional range) can be given approximately by:

$$\frac{1}{R} = 0.046\ U_a \quad , \qquad (23)$$

where the surface wind speed is in knots and R is in centimeters. The range of observed linearity was between 8 knots (where waves began to be formed) and 20 knots over a fetch of 26 inches.

Turning now to the fourth moment m_{4o}, obtained by setting r = 2 in (20), we see that:

$$m_{4o} = \frac{3a}{8q\ g^4} \left[\frac{b}{U_a}\right]^{9-p} \Gamma\left(\frac{p-9}{q}\right) \quad . \qquad (24)$$

It follows that for p = 6, the Neumann spectrum case, the exponent of b/U_a is 3 so at once it is evident that m_{4o} becomes infinite for $U_a = 0$. Moreover m_{4o} decreases as the inverse third power of wind speed. These observations show that on this level the Neumann spectrum at last meets its limit of validity in the capillary region, since, according to Schooley's observations cited above, gaussian curvature should increase as the square of the wind speed U_a. Any gamma-type model which has p = 11 would exhibit this feature observed by Schooley. However, then m_{2o} for this model (cf. (22)) would not have the observed linear behavior with wind speed. These observations reinforce our earlier conclusion that gamma-type one-dimensional spectra are only first approximations to a more complex analytical spectral formula as yet to

be determined over the *whole* frequency spectrum, and which completely describes the structure of the dynamic air-water surface. It must also be borne in mind that empirical laws such as the wave-slope wind-speed law and the curvature law (23) against which the gamma spectra have been pitted are determined only for limited wind speed ranges and wave length ranges. Thus what may be a linear law in one range of wind speed could very well blossom into a polynomial law in wind speeds over a greater range; and perhaps ultimately a rational function in wind speeds (i.e., a ratio of two polynomials) is forthcoming which (e.g.) eventually goes to zero with increasing wind speeds. (The sea is blown smooth in the limit.)

Wind Speed, Wavelength, and Wave Energy

We close this discussion of models of ocean wave spectra by combining the Neumann spectrum with the Kelvin-Helmholtz wave theory, the purpose being to predict the relative energy dependence of such waves on wind speed or wave length. Thus, from (98) of Sec. 12.3 we have (using wave height H)

$$\mathcal{E}(k) = \frac{1}{8}\,\rho\,H^2\,g + \frac{T_1}{16}\,H^2\,k^2$$

for the energy of a sinusoidal wave with wave number k and height H, and which is propagated jointly by surface tension and gravity forces. If we have a continuum of waves in which $(1/8)\,H^2(\tau)$ is replaced by T_τ (as in (7)) or $(1/8)\,H^2(k)$ is replaced by T_k, then by the same kind of reasoning that led to (8a):

$$\mathcal{E}(k_1,k_2) = \rho\,g\int_{k_1}^{k_2} T_k\,dk + \frac{T_1}{2}\int_{k_1}^{k_2} k^2\,T_k\,dk \qquad (25)$$

is the energy content per unit horizontal surface area of the set of waves with wave numbers in the interval $[k_1,k_2]$. In particular, on recalling (116) and (121) of Sec. 12.4, the total energy for Kelvin-Helmholtz waves, under an isotropic direction spectrum, is:

$$\boxed{\mathcal{E} = \rho g\,m_{oo} + T_1\,m_{2o}} \quad . \qquad (26)$$

If the Neumann spectrum is used for the waves, then from (10) and (11), we can write (26) as:

$$\mathcal{E} = C_1\,U_a + C_2\,U_a^5 \quad , \qquad (27)$$

where we have written:

$$\text{"}C_1\text{"} \quad \text{for} \quad \frac{T_1 C\pi^3}{4g}\sqrt{\frac{\pi}{2}} \tag{28}$$

and:

$$\text{"}C_2\text{"} \quad \text{for} \quad \frac{3}{32}\frac{\rho C\pi^3}{g^2}\sqrt{\frac{\pi}{2}} \quad . \tag{29}$$

It turns out that, on using $T_1 = 74$ dynes/cm,

$$\begin{aligned} C_1 &= 6.1 \times 10^{-4} \text{ dyne cm}^{-2} \text{ sec} \\ C_2 &= 3.2 \times 10^{-9} \text{ gm cm}^{-5} \text{ sec}^3 \quad . \end{aligned} \tag{30}$$

In the cgs system, so that U_a is in centimeters per second and $\mathcal{E}$ in ergs per centimeter squared.

From (27) we can see that for small winds, i.e., $U_a << 1$ (in whatever units) the linear power of U_a will be *relatively* dominant, so that capillary waves will contribute most of the energy $\mathcal{E}$. For greater winds, i.e., $U_a >> 1$, the fifth power of U_a takes dominance, and gravity waves will hold the lion's share of energy. In this way we have made quantitative the intuition we already possessed about the energy $\mathcal{E}$ in our discussions of (98) of Sec. 12.3.

<< Table of Contents << Title Page >> Next Page >>

12.9 Theoretical Wave Spectra Models

In this section we shall review some of the empirical data and models discussed in Secs. 12.5-12.8 from a relatively theoretical vantage point with the purpose in mind of "rationalizing" the empirical results and embedding them in a plausible conceptual framework. In particular, we shall show how one can view the gaussian frequency distributions of wave elevations and slopes as the result of the steady confluence of great numbers of independent simple wave events. Some of the wave spectra of Sec. 12.8 can also be viewed in this way. However, a matter which cannot yet be so simply viewed is the *generation process* of the wave spectra. The mathematical description of this process is still incomplete. Some current approaches to this description problem will be outlined in the closing paragraphs of this section.

The Wave Elevation Distribution

Experimental evidence for the gaussian form of the distribution of wave crest elevations about a mean sea level under open sea, steady state wind conditions is now largely established (cf., e.g., Fig. 12.46). We can construct a simple mathematical basis for this empirical fact as follows. Imagine a uniformly graduated vertical pole fixed into the sea bottom and visualize the wave profile moving up and down along the pole as the waves go by (Fig. 12.53). Suppose that